Lithium *tert*-Butyl[phenyl(2,2,6,6-tetramethylpiperidino)boryl]amide: A Versatile Reagent[‡]

Ulrike Braun,[a] Tassilo Habereder,[a] and Heinrich Nöth*[a]

Dedicated to Professor Nils Wiberg on the occasion of his 70th birthday

Keywords: Lithium *tert*-butyl[phenyl(2,2,6,6-tetramethylpiperidino)boryl]amide / *N*−Metal borylamides

A new synthesis of tmp(PhB)N(*t*BuNLi) (**1**, tmp = 2,2,6,6-tetramethylpiperidino) is presented. Compound **1** reacts with many group 13–15 halides, as well as with BH_3·THF, to afford, in most cases, compounds of the type tmp(PhB)N*t*Bu–ER_{n-1} (E = B, Al, Ga, In, Ge, Sn, P, As, Sb, and R = H, Me, Hal). The borane, alane, gallane and indane derivatives have cyclic structures, as shown by X-ray structure determinations, whereas ER_{n-1} = $GeCl_3$, $SnMe_3$, $SnMe_2Cl$, SnCl, catecholatophosphanyl, $AsCl_2$ and $SbCl_2$ are noncyclic, although the arsane and stibane derivatives show weak intramolecular E–N coordination to the tmp–N atom.

Introduction

Although *N*-lithioaminoboranes are well known and have been used in the synthesis of various types of aminoboranes, those of type **B** can be compared with amidines (**A**) and amidates (**C**); solid-state structures of their alkali metal salts of the latter are available.[2−5] The first structurally characterized amidine was the trimethylsilyl derivative $PhC(=NSiMe_3)N(SiMe_3)_2$.[6] Since then, the chemistry of amidines and amidinates has been extended into transition metals chemistry.[7,8] It is, therefore, of interest to compare the chemistry of alkali metal compounds containing type **B** anions with that of the carbon analogs. The former can also be seen as a special type of N−metal borylamides.

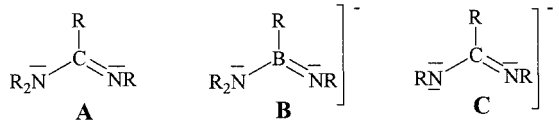

The structures of *N*-lithioborylamides[9−13] have been determined relatively recently, although some were used as reagents much earlier. The first reaction of an *N*-lithioaminoborane was reported by Dewar at al.[14] [Equation (1)]. Borazinylborazines have been obtained from N-lithioborazines and chloroborazines by Wagner and Bradford,[15] while both symmetrically and asymmetrically substituted diborylamines resulted from reactions of $R_2B-NR'Li$ and R''_2BCl.[16] Moreover, by using $PhB(NRLi)_2$ [17] a series of four-membered rings containing metal atoms, $M(NR)_2BPh$, as well as spirocyclic compounds, $M[(NR)_2BPh]_n$, have been obtained.[18] As reported in the preceding paper, many asymmetrically substituted diborylamines and metallated diaminoboranes of the type tmp−BX−$NCMe_3$−EX_{n-1} (tmp = 2,2,6,6-tetramethylpiperidino, E = B, Al, Ga, In, Si, Sn, Li, Mg, Zn, Cd; X = H, Me, Bu, Ph, Cl, Br) are accessible.[1] Among these is the stable lithium borylamide tmp−BPh−$NCMe_3Li$·OEt_2 (**1**), which offered itself as a reagent for further synthesis. The anion **B** of this compound is isoelectronic and isolobal with **A**.

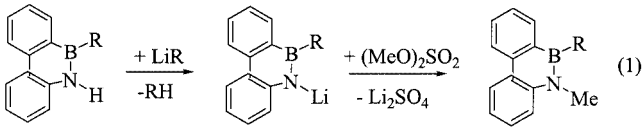

Results

Reactions of tmp−BPh−N(CMe$_3$)Li with Group 13 Compounds

Although the lithium compound **1** can be readily prepared by the addition of LiPh to the aminoiminoborane tmp−B=N−CMe_3 [1] we were looking for a more convenient synthesis, circumventing the isolation of the amino-

[‡] Contribution to the Chemistry of Boron, 254. Part 253: Ref.[1]

[a] Department of Chemistry, University of Munich, Butenandtstr. 5−13, 81377 München, Germany
E-mail: H.Noeth@lrz.uni-muenchen.de

iminoborane. Consequently, we developed a one-pot synthesis of **1** according to Equation (2). Yields are almost quantitative, and the resulting suspension of LiCl in the solution of **1** can be used directly for further synthesis.

The reaction of **1** with BH_3·THF in THF requires 2 equivalents of the borane reagent as the LiH formed as an intermediate reacts with the borane component to produce $LiBH_4$ [Equation (3)].[19] A 1:2 stoichiometry is also necessary for the quantitative conversion of **1** into the difluoroborane derivative **3**. The cyclic nature of **2** and **3** is proven by two ^{11}B NMR signals for a tricoordinate and a tetracoordinate boron atom as well as by X-ray structure determinations (see below).

Although boron halides cleave the CO bonds of ethers, no ether cleavage was observed in the reaction of **1** with *B*-(chloro)catecholborane, see Equation (4). The resulting borylated diaminoborane **4** is cyclic, as evidenced by ^{11}B NMR spectroscopy and the determination of its molecular structure. However, **1** did not react at ambient temperature with $tmpBCl_2$, tBuNHBCl_2, 2,4,6-trichloroborazine, and tB$uBCl_2$ in non-polar solvents.

Dimethylchloroalane, -gallane and -indane are dimeric in nonpolar solvents and may, therefore, be less likely to be attacked by **1** as a nucleophile. However, in the presence of diethyl ether, mononuclear species $Me_2ECl\ OEt_2$ form that may react with **1**. Indeed, reactions according to Equation (**7**) proceed readily to yield compounds **7**–**9**, all of which were shown to be cyclic by NMR spectroscopic data and X-ray structure determinations.

To synthesize noncyclic tmp–BPh–$NCMe_3$–AlX_2 compounds we treated the bulky monomeric bis(amino)chloroalane tmp_2AlCl [20] with **1**. The reaction was expected to proceed according to Equation (5). However, the only product we could isolate, in very low yield, was compound **8**, the tmpH solvate of tmp–BPh–$NCMe_3Li$. No LiCl precipitated.

After refluxing the mixture, the ^{11}B NMR spectrum exhibits a new signal at $\delta = 35.7$ ppm in addition to that of **1** in a 1:1 ratio, and a new broad ^{27}Al signal at $\delta = 82$ ppm. The isolated compound **6** shows practically the same NMR spectroscopic data as **1**, with additional signals for tmpH in the ^1H NMR spectrum.

Because the reaction was performed under strictly anhydrous conditions, we exclude the formation of tmpH by hydrolysis of tmp_2AlCl. Therefore, we assume that tmpH is formed by ether cleavage, as suggested in Equation (6). To test this hypothesis we kept an ether solution of tmp_2AlCl under reflux. While tmp_2AlCl shows a ^{27}Al NMR signal in

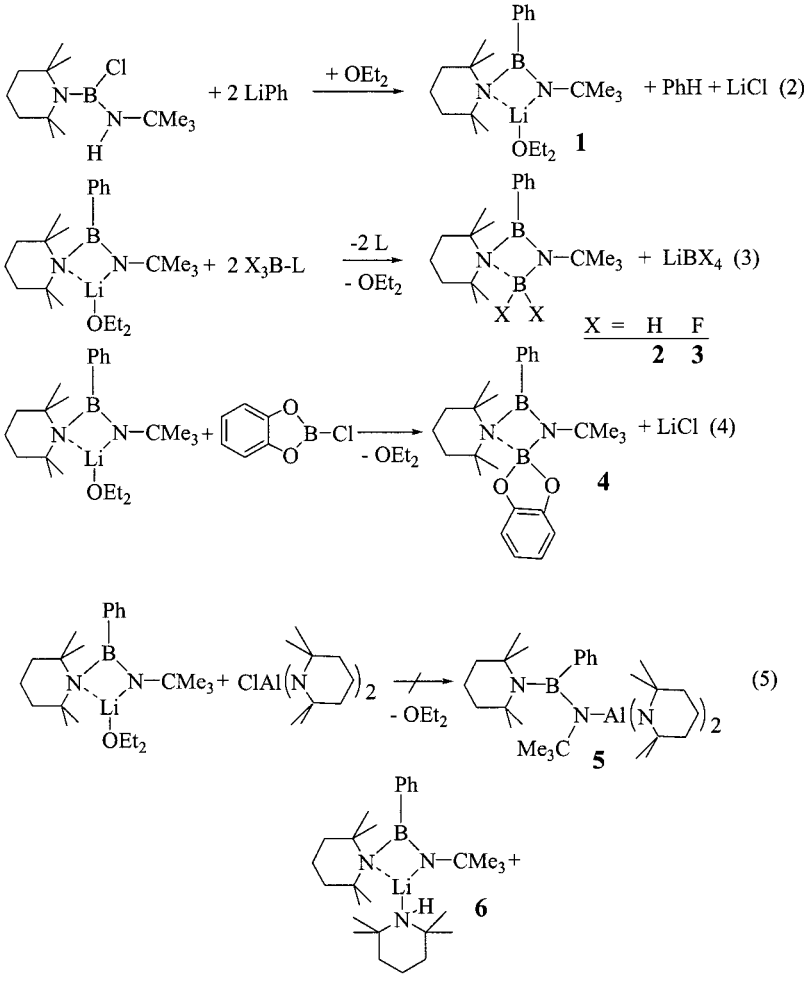

$$(tmp)_2AlCl + OEt_2 \longrightarrow tmpAl(Cl)OEt + tmpH + C_2H_4 \quad (6)$$

hexane at δ = 134 ppm, ($h_{1/2}$ = 13 700 Hz), the ether solution, after heating for some time, exhibits two additional signals at δ = 112.8 and 82 ppm. The first of these results from $tmp_2AlCl{\cdot}OEt_2$,[21] while the second corresponds with dimeric tmpAl(OEt)Cl.[22] Although pure compounds could not be isolated, the data indicate that the assumption of ether cleavage by tmp_2AlCl is not unjustified.

We have not yet studied the interaction of **1** with $AlBr_3$, $GaCl_3$ and $InCl_3$ to see whether more than one halogen atom can be replaced by the anion of **1** in the formation of chelates where the coordination number of the metal atom could increase up to six.

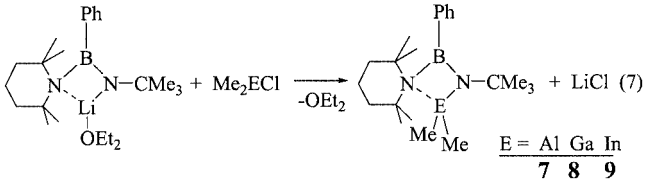

Spectra

Table 1 summarizes the ^1H, ^{11}B and ^{13}C NMR spectroscopic data of compounds **2**–**4** and **6**–**9**. Compound **6**, which is akin to **1**, shows a sharper ^{11}B signal than **1**, and a somewhat deshielded boron nucleus. Protons of the CMe_2 groups of the tmp substituent are better shielded than those of the coordinated tmpH molecule, although both nitrogen atoms are tetracoordinate. Proton signals of the CH_2 groups overlap (H2,3,4), while in **1** the protons at C2/4 and C3 are nicely separated triplets and multiplets.[1] Moreover, there is only one set of ^{13}C resonance each for the two tmp units in **6**. Thus, in solution the molecule is fluxional.

^{11}B resonances of the tricoordinate boron atom of **2**–**4** are shifted to lower field compared with **1**. This mirrors the influence of the charge withdrawal from the BN bonds as the substituents at the tetracoordinate B atom become more electronegative. The coupling constants $^1J(^{11}B^1H)$ and $^1J(^{19}F^{11}B)$ are similar to those in the corresponding 1,3,2,4-diazadiboretines.[23] Moreover, the difference in chemical shifts for the two ^1H and ^{13}C resonance of atoms H6,7 and C6,7 increases from **2** via **3** to **4**. The data confirm that the cyclic nature of these compounds is retained in solution.

Conversely, the ^{11}B shielding for the PhB boron atom is almost uninfluenced by the heteroatoms Al, Ga, and In in **7**–**9**. For the indium compound **9**, only a single resonance appears in the ^1H and ^{13}C NMR spectrum for H6,7 and C6,7, respectively. This indicates that, in solution, the In1–N1 bond is opened, while it is present in the solid state. That its structure in solution differs from that of **7** and **8** becomes apparent from the low field ^{13}C resonance of atoms C1,5. This deshielding is still noticeable for C2/4 and C3.

The fragmentation of compounds **2** and **3** in the mass spectrum starts from the molecular ion, which has a 100% relative intensity for the boron hydrogen compound **2**, but only 4.5% for the fluoroborane derivative **3**. In both cases, a methyl group is lost in a first step, which most likely comes from breaking the respective bond at the tmp unit (62 and 100% relative intensity, respectively). Strong peaks appear for ions ($M^+ - CMe_3$) (28 and 82%). Moreover, ions derived from the imino borane are also readily detected, as shown by fragments $tmp{-}B{=}NCMe_3^{+\cdot}$, $tmpB{-}Ph^+$, and $PhB{=}NCMe_3^+$. Loss of a tmp radical from $M^{\cdot+}$ can also be noted.

Fragmentation of the Al and Ga compounds **7** and **8** is characterized by strong peaks for the [M^+ − Me] ions (100 and 43%, respectively) where the E–C bonds of Al and Ga are broken. In addition, a [$M^+ - CMe_3$] peak appears for **7** (21.5%) but not for **8**. Also, fragments [$tmp{-}EMe^+$] are observed (100%, 42%), showing the preferred formation of $Me_3C{-}N{=}B{-}Ph$ in the fragmentation process, which is a stable leaving group. In contrast, fragmentation to give [$tmp{-}B{-}Ph^{\cdot+}$] is less favored because this would generate molecules $MeE{=}NCMe_3$, which are, most likely, not as stable as an imino borane unit.

Molecular Structures

The molecular structures of **2**–**4** and **6**–**9** were determined by X-ray structure analysis. Table 2 contains selected and relevant structural parameters. The molecular structures of **2**–**4** and **6**–**8** are depicted in Figure 1–6, respectively; data for compound **1** are added for comparison with **1·tmpH** (= **6**). In all cases, these compounds feature a four-membered ring.

Table 1. NMR spectroscopic data of compounds **2**–**4** and **6**–**9;** δ in ppm, coupling constants and line widths in Hz

	$\delta^{11}B$	δ^1H H2,4,3	H6,7	CMe_3	$\delta^{13}C$ C1,5	C2,4	C3	C6,7	C10	C11–13
BH_2, **2**	32.7, −4.3 t[a]	1.25–1.50 m	1.39, 1.70	1.23	57.5	37.0	17.1	27.0, 30.4	50.6	31.0
BF_2, **3**	35.7, 4.8 t[b]	1.28–1.56 m	1.49, 1.70	1.26	58.3	38.2	16.9	26.9, 31.9	51.5	32.0
CatB, **4**	35.9, 13.4	1.08–1.52 m	1.21, 1.91	1.17	57.7	38.1	16.9	27.2, 38.1	51.3	31.8
LitmpH, **6**	35.5	1.18–1.68 m	1.06, 1.29,	1.00	58.2, 59.3	38.1, 38.4	16.1, 18.6	33.3, 33.4	49.4	31.8
$AlMe_2$, **7**	36.5[c]	1.30–1.53 m	1.29, 1. 69	1.11	56.3	36.3	17.0	30.5, 32.8	51.1	33.6
$GaMe_2$, **8**	36.7[d]	1.28–1.57 m	1.25, 1.69	1.10	56.2	36.2	17.3	30.9, 32.8	51.7	33.7
$InMe_2$, **9**	35.0[e]	1.55 t, 1.69 m	1.20	1.00	65.9	38.1	18.9	37.5	52.4	33.4

[a] $^1J(^{11}B^1H)$ = 107. [b] $^1J(^{19}F^{11}B)$ = 48. [c] $h_{1/2}$ = 183. [d] $h_{1/2}$ = 137. [e] $h_{1/2}$ = 234.

Table 2. Selected bond lengths (Å) and bond angles (°) of **2**−**4** and **6**−**9**

Compound	**1**·OEt_2	**1**·tmpH (**6**)	**2**	**3**	**4**	**7**	**8**	**9**
B1−N1 (Å)	1.564(4)	1.571(4)	1.593(4)	1.588(4)	1.584(2)	1.600(4)	1.593(3)	1.580(4)
B1−N2	1.361(4)	1.371(4)	1.370(3)	1.376(3)	1.369(2)	1.380(4)	1.377(3)	1.375(3)
B1−C14	1.617(4)	1.617(3)	1.586(3)	1.587(4)	1.583(2)	1.597(5)	1.596(4)	1.606(4)
N1−C1	1.528(3)	1.503(3)	1.539(2)	1.551(2)	1.547(2)	1.539(3)	1.544(3)	1.528(3)
N1−C5	1.526(3)	1.496(3)	1.539(2)	1.551(3)	1.552(2)	1.551(3)	1.532(3)	1.526(3)
N2−E	1.884(5)	1.883(5)	1.555(3)	1.523(4)	1.512(2)	1.869(2)	1.935(2)	2.137(2)
N1−E	2.085(6)	2.157(4)	1.665(3)	1.689(3)	1.741(3)	2.078(2)	2.175(2)	2.376(2)
N2−C10	1.467(4)	1.460(3)	1.463(3)	1.475(3)	1.483(2)	1.483(3)	1.474(3)	1.476(4)
X−E (X=O, C)	1.929(5)	2.155(5)	1.15(2)	1.383(2)	1.460(2)	1.977(3)	1.990(3)	2.170(3)
N1−B1−N2 (°)	112.9(2)	113.6(2)	96.8(2)	97.2(2)	86.2(1)	105.7(2)	106.6(2)	109.3(2)
N1−B1−C14	120.9(3)	124.7(2)	130.3(2)	130.7(2)	130.3(1)	126.0(2)	125.7(2)	125.1(2)
N2−B1−C14	126.1(3)	124.8(3)	132.8(2)	132.2(2)	131.8(2)	128.3(2)	127.6(2)	125.6(3)
B1−N2−E	91.6(2)	93.4(2)	93.9(2)	94.2(2)	95.8(1)	97.2(2)	98.9(2)	100.7(2)
B1−N1−E	78.9(2)	78.2(2)	82.1(2)	80.9(2)	80.0(1)	82.8(2)	83.3(2)	85.5(1)
N1−E−N2	75.7(2)	74.9(2)	87.2(2)	87.7(2)	86.2(1)	73.92(9)	70.8(1)	64.39(7)
B1−N2−C10	129.7(2)	129.2(2)	137.3(2)	136.2(2)	135.4(1)	131.4(2)	132.6(2)	131.9(2)
E−N2−C10	138.5(3)	137.3(2)	128.8(2)	129.6(2)	128.7(1)	131.1(2)	128.1(2)	127.3(2)
C1−N1−C5	116.2(2)	115.0(2)	114.5(2)	114.2(4)	114.2(1)	113.0(2)	113.3(2)	114.2(2)
X−E−X			112.6(2)	107.3(2)	105.7(1)	105.9(4)	109.6(3)	114.0(1)

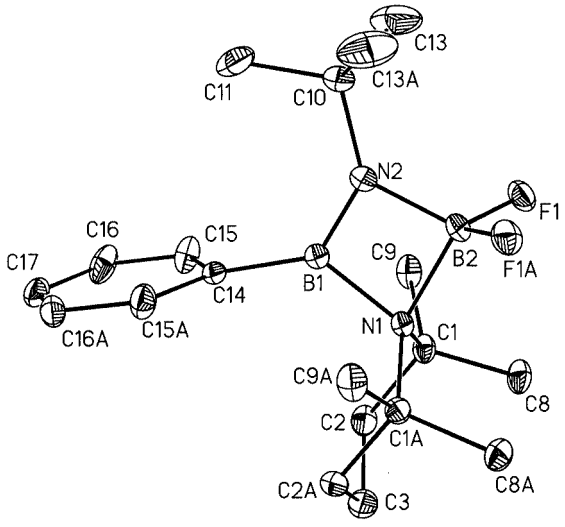

Figure 1. Molecular structure of compound **2**

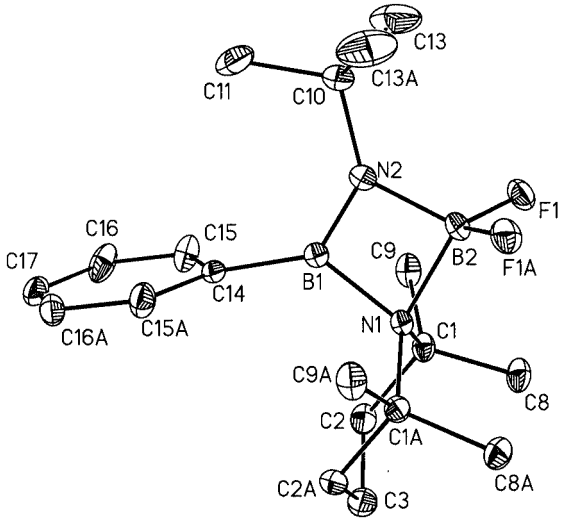

Figure 2. Molecular structure of compound **3**

B1, B2, N1, N2, C14, C17, C10 and C13 of compounds **2** and **3** sit on a mirror plane in the orthorhombic unit cell. The four-membered ring is planar and the phenyl group as well as the C1−N1−C1A unit of the chair-shaped tmp ring stand orthogonal to the ring plane. The B2−N1 bond length of the tetracoordinate atoms increase in the order $BH_2 < BF_2 <$ Bcat. This can be attributed to inductive effects, which are also mirrored in the B2−N2 bond length (H > F > OR). As expected, the B1−N2 bond is shorter, by about 0.2 Å, than the B1−N1 bond because the bond to N1 is a single bond to a tricoordinate boron atom. Moreover, the B2−N1 bond is even longer in both compounds [1.665(3) and 1.689(3) Å, respectively]. Compound **3** is isostructural with **2**; its B1−N1 bond is shorter than in **2** by

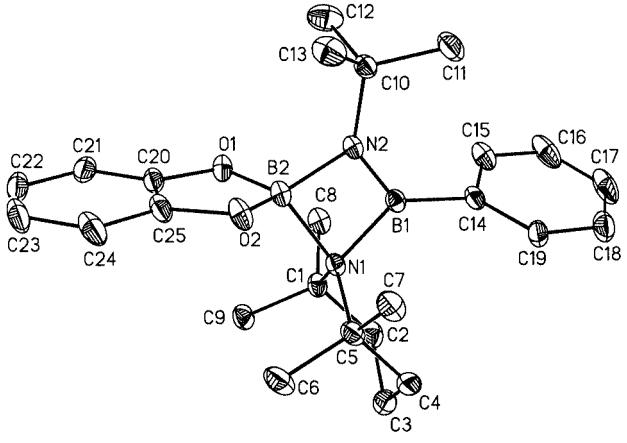

Figure 3. Molecular structure of compound **4**

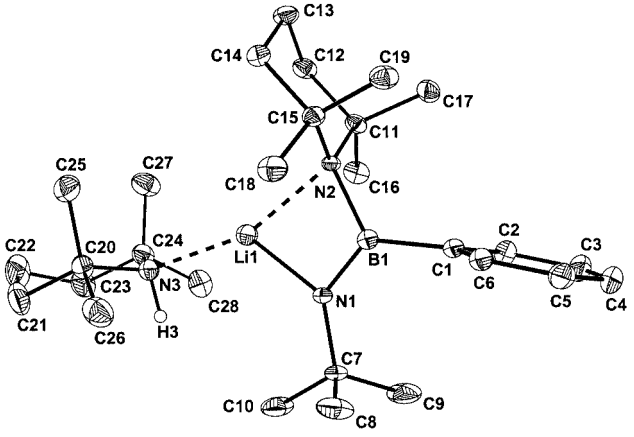

Figure 4. Molecular structure of compound **6**

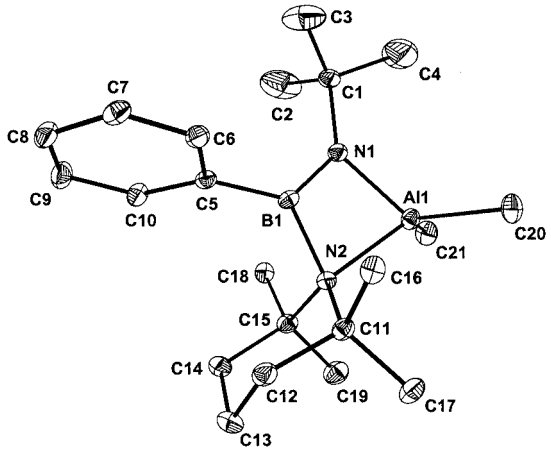

Figure 5. Molecular structure of compound **7**

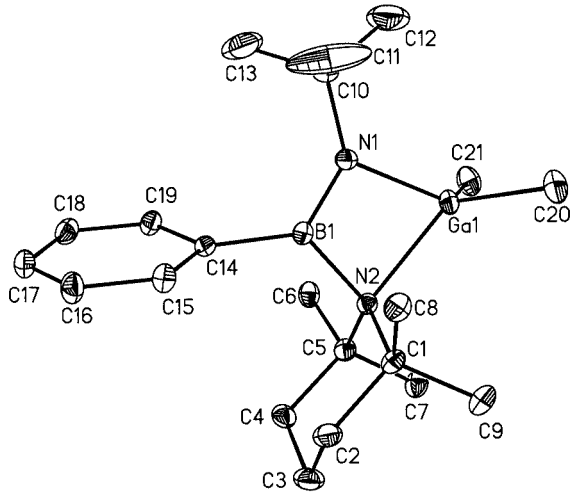

Figure 6. Molecular structure of compound **8**

0.006 Å but the B1−N2 bond is 0.009 Å longer. The B2−N2 bond is significantly shorter [1.523(4) Å] in **3** than in **2** [1.555(3) Å]. Bond angles at the boron atoms in these two compounds are more open than at the nitrogen atoms, and the N−B−N bond angle at the tetracoordinate boron atom is almost 10° smaller than at the tricoordinate boron atoms B1.

While the B1−N1 bond lengths decrease by 0.019 Å when moving from the aluminium compound **7** to the indium compound **9**, the B1−N2 bond lengths remain unaffected by the heavy group 13 atoms. However, the effect of these atoms leads to a shrinking of the N1−C1/5 bonds on moving from Al to In. There is a wider N1−B1−N2 bond angle for the indium compound [109.3(2)°] than in the aluminum derivative [105.9(3)°]; this can be attributed to the lengthening of the E−N1 bond from 2.079(3) Å in **7** to 2.376(2) Å in **9**.

As expected, the E−N2 bond lengths for the pair **7**/**9** also increase, but the difference is larger (0.298 Å) than for E−N1 (0.268 Å).

The four-membered ring of **7** is not planar. The molecule shows an interplanar N1−B1−N2/N1−Al1−N2 angle of 6.3°. In contrast, the ring of **8** is planar; nevertheless, its phenyl group is not perpendicular to the N1B1N2 plane but is twisted about the B1−C14 bond by 74.3°. The same twisting is found for the indium compound **9**. While the C_2E (E = Al, Ga, In) units stand orthogonal or almost perpendicular to the N1−E−N2 plane the C1−N1−C5 planes deviate from orthogonality with respect to the B1−N1−E plane by 4° for **7** and by 3.4° for **9**.

Reactions of tmp−BPh−N(CMe$_3$)Li with Group 14 Compounds

Particularly for steric reasons, the reactions of **1** with halides of group 14 should be less favored than with group 13 halides. Indeed, neither Me_3SiCl nor Ph_3SiCl reacted with **1**. However, $SiCl_4$, a stronger Lewis acid than the R_3SiCl compounds, reacts according to Equation (8) with the formation of tmp−BPh−N*t*Bu−$SiCl_3$. Such compounds can also be obtained from tmp−BPh(Cl) and LiN(CMe$_3$)(SiMe$_3$) in the presence of toluene [Equation (9)]. However, in addition to **10**, tmpBPh(Tol) is formed [Equation (10)]. The two compounds could not be separated by crystallization. Obviously, Li(tol) results from the solvent toluene that is metallated by the lithium amide, a not uncommon reaction.[24]

Like Me_3SiCl, the methylhalogermanes Me_3GeCl and Me_3GeBr are unreactive towards **1**, but $GeCl_4$, like $SiCl_4$, afforded the trichlorogermyl derivative **11** [Equation (11)], but reflux conditions in hexane are required. In contrast, **1** and Me_3SnCl interact easily to produce the trimethylstannyl derivative **12**, and reaction with Me_2SnCl_2 afforded compound **13**. However, an attempt to use Me_2SnCl_2 to attach two diaminoborane units to the Me_2Sn fragment [Equation (13)] was not successful − only monosubstitution was observed. In addition, on heating, decomposition occurred to give the diazadiboretidine (tmpB−N*t*Bu)$_2$, which was detected by ^{11}B NMR spectroscopy.[23] All these metallated diaminoboranes of type tmp−BPh−N*t*Bu−EX_n (E = Ge, Sn), **11**−**13**, are noncyclic (see below). No reactions were noted between **1** and Ph_3GeCl, Ph_3SnCl, and Ph_3PbCl in the presence of hexane, most likely due to steric reasons.

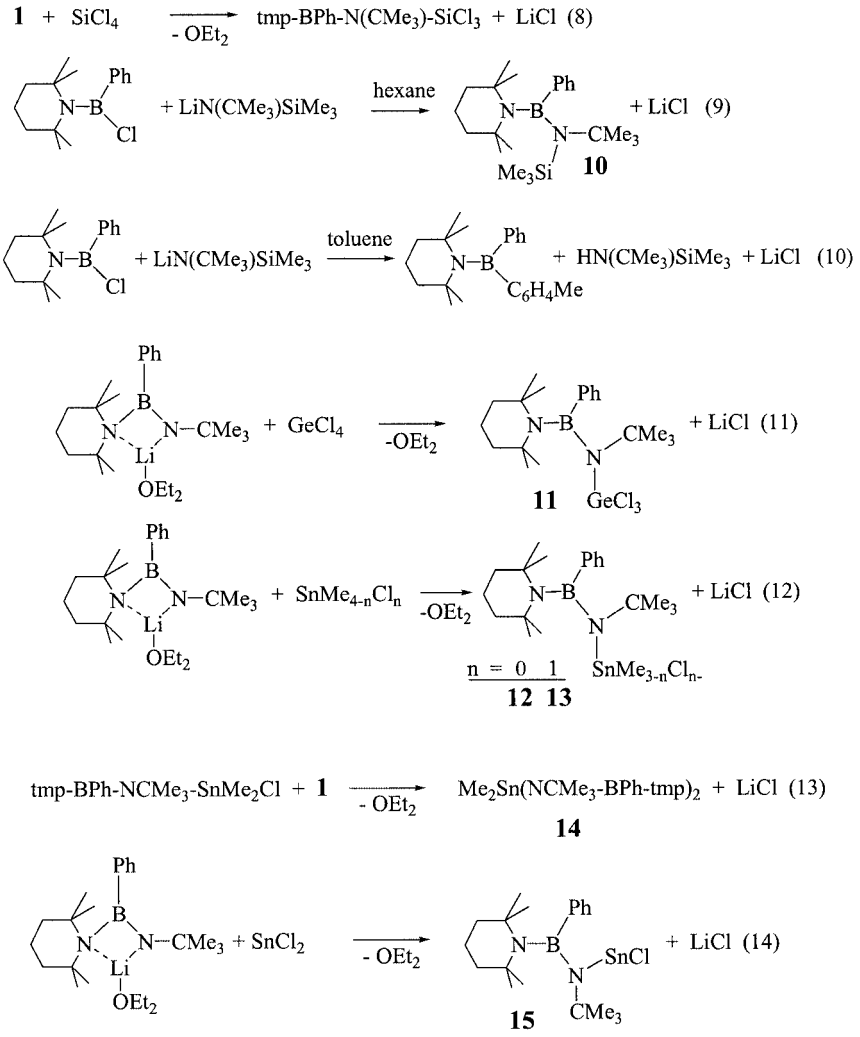

Similarly, only a single Cl atom of $SnCl_2$ could be replaced by the tmpBPh−N*t*Bu group [Equation (14)]. No ^{119}Sn resonance signal was detected for **15**, but $\delta^{11}B = 38.0$ ppm agrees with a metallated diaminoborane. In the gas phase, no mass higher than M^+ was found for **15**, suggesting that the compound is most likely monomeric in solution. No single crystals could be obtained, and, therefore, it was not possible to determine its solid-state structure.

NMR Spectra

In the NMR data of **11**−**13** and **15** (Table 3) the shielding of the ^{11}B nuclei is practically identical and at lower field than with the cyclic species **2**−**9**. In contrast to the latter, the N1 atoms reside in a planar environment and, therefore, can be considered to be sp^2 (see below). Since there are two NMR signals for the CMe_2 groups in the ^1H and ^{13}C NMR spectra there must be a hindered rotation about the B1−N1 bond. Indeed, the interplanar angle CN1C5/N1B1N2 is only 30° for the $GeCl_3$ compound; these angles are 118.3° and 117.7° for the tin compounds **12** and **13**. Therefore, B1−N1 π-bonding should not be pronounced in **12** and **13**. For **11** there may be hindered rotation about the B1−N1 bond due to steric hindrance. Cl substitution at Ge and Sn leads to a deshielding of the protons of the *t*Bu groups but this is not reflected in the ^{13}C resonances of either C10 or C11 to C13. In particular, the ^{13}C resonances for C1 and C5 fall in the same range as those for the cyclic species; however, those of C6/7 seem to be less well shielded. Thus, these data do not allow us to decide whether these compounds are cyclic or noncyclic. However, $\delta^{119}Sn$ for **12** and **13** are $\delta = 17.9$ and 93.1 ppm, indicating the presence of a tetracoordinate tin atom.[25] In particular, the tin resonance of **13** falls well within the range found for similar compounds [13,25] while the ^{119}Sn resonance of **12** corresponds well with that of $Me_3Sn(tBu)N-BH-tmp$ ($\delta^{119}Sn$ = 27.4),[21] 2-[trimethylsilyl(trimethylstannyl)amino]pyridine ($\delta^{119}Sn$ = 10.2 ppm),[26] and 8-[bis(trimethylstannyl)amino]-quinoline ($\delta^{119}Sn$ = 26.4).[27] Unfortunately, we were unable to record a ^{119}Sn spectrum for the tin(II) compound **15**. Since its ^1H, ^{11}B and ^{13}C NMR spectroscopic data are rather similar to those of the other two tin compounds we assume that this molecule is not associated (e.g. dimeric or trimeric). In accord with this, its mass spectrum shows the parent peak as the highest mass.

Table 3. NMR spectroscopic data of **11**−**13** and **15**−**18**; δ (ppm), line widths $h_{1/2}$ (Hz)

	$\delta^{11}B$	$\delta^{1}H$ H2,4,3	H6,7	CMe_3	$\delta^{13}C$ C1,5	C2,4	C3	C6,7	C10	C11−13
$GeCl_3$,**11**	39.4 [a]	1.46−1.58 m	1.35, 1.41	1.21	56.8	38.8	15.9	34.2, 35.1	51.6	33.8
$SnMe_3$, **12**	39.8 [b]	1.39−1.64 m	1.17, 1.43	1.51	56.2	41.1	18.4	30.1, 35.1	52.4	34.9
$SnMe_2Cl$, **13**	39.8 [c]	1.39−1.64 m	1.02, 1.06	1.30	56.0	41.0	18.0	30.9, 36.3	52.1	35.6
SnCl, **15**	38.0 [d]	1.36−1.58 m	1.13, 1.29	1.13	53.4	38.9	17.6	31.9, 33.8	53.4	33.6
Pcat, **16**	40.5 [e]	1.42−1.66 m	1.37, 1.51	1.13	55.9	38.2	16.1	34.1, 34.6	58.7	33.3
$AsCl_2$, **17**	41.3 [f]	1.15−1.44 m	1.10, 1.48	1.53	55.3	38.8	17.7	30.8, 33.7	62.7	33.5
$SbCl_2$, **18**	42.7 [g]	1.12−1.33 m	1.05, 1.11	1.54	55.4	38.0	17.6	29.0, 33.7	60.6	34.3

Line widths: [a] 209. [b] 209. [c] 260. [d] 330. [e] 358. [f] 220. [g] 222.

Molecular Structures

Selected structural parameters for **11**−**13** are summarized in Table 4, and the structures of these compounds are depicted in Figures 7−9, respectively. In all these compounds the sum of bond angles at N1 is close to 360°, demonstrating that the atoms N1 are of sp^2 type. Therefore, this atom may form BN π-bonds with atom B1 in addition to atom N2.

Surprisingly, the B1−N1 bond of the trichlorogermyl compound **11** is significantly shorter than the B1−N2 bond [1.422(4) vs. 1.510(4) Å]. Inspection of the respective interplanar angles gives a value of 30.3° for C1N1C5/N1B1N2 and 60.5° for GeN2C10/N2B1N1. Therefore, the tmp group is better suited for BN π-bonding. The N1−B1−N2 bond angle of 123.3(3)° accords with the noncyclic structure. Another feature of interest is that one of the three Ge−Cl bond lengths is about 1% shorter than the other two. However, there is no apparent significant H···Cl interaction (all distances are longer than 3.35 Å) that would explain this deviation. The arrangement of the Ge1−N2−B2−N1 chain is *cisoid* in the solid state.

In contrast, the methylstannyl compounds **12** and **13** show a *transoid* arrangement for the Sn1−N2−B1−N1 chain. In **12** the B1−N1 bond is longer [1.475(5) Å] than the B1−N2 bond [1.430(4) Å], in agreement with interplanar angles of C1N1C5/N1B1N2 (116.4°) and C10N2Sn1/N2B1N1 (32.2°). The phenyl group is twisted against the N1B1N2 plane by 44.1°. B1 and N2 reside in a planar environment, as is also found for the chlorodimethylstannyl compound **13**. The B1−N1 bond in **13** is 0.01 Å shorter than in **12**, while the B1−N2 bond in **13** is 0.008 Å longer than in **12**. Such differences arise from the differ-

Table 4. Selected bond lengths (Å) and bond angles (°) of **11**−**13** and **16**−**18**

	$GeCl_3$, **11**	$SnMe_3$, **12**	$SnMe_2Cl$, **13**	Pcat, **16**	$AsCl_2$, **17**	$SbCl_2$, **18**
B1−N1	1.422(4)	1.475(5)	1.465(4)	1.431(4)	1.496(5)	1.527(2)
B1−N2	1.510(4)	1.430(4)	1.438(4)	1.530(5)	1.428(4)	1.411(2)
B1−C14	1.587(5)	1.601(5)	1.613(4)	1.596(5)	1.591(6)	1.595(3)
N2−C10	1.513(4)	1.505(3)	1.511(3)	1.535(5)	1.526(4)	1.516(2)
N1−C1	1.539(4)	1.498(4)	1.506(3)	1.539(5)	1.527(4)	1.534(2)
N1−C5	1.531(4)	1.501(4)	1.505(3)	1.531(5)	1.526(4)	1.535(2)
N2−E	1.796(2)	2.103(3)	2.081(2)	1.760(3)	1.872(3)	2.072(2)
E1−X1 (O, Cl)	2.1203(9)	2.140(3)	2.4016(8)	1.715(3)	2.292(1)	2.3899(6)
E1−X2 (O, Cl)	2.1312(9)	2.145(5)	2.122(3)	1.704(3)	2.234(1)	2.4809(7)
E1−N1	3.507	4.373	4.328	3.174	2.516(3)	2.539(1)
N1−B1−N2	123.3(3)	126.8(3)	128.1(2)	121.4(3)	111.3(3)	110.3(2)
N2−B1−C14	111.9(3)	113.1(3)	113.3(2)	114.7(3)	122.4(3)	123.8(2)
N1−B1−C14	124.7(3)	119.0(3)	118.5(2)	123.8(3)	126.2(3)	125.8(2)
B1−N2−E1	117.2(2)	116.2(2)	113.0(2)	106.0(2)	103.0(2)	102.4(1)
B1−N2−C10	121.3(2)	127.9(3)	128.8(2)	122.5(3)	128.3(3)	128.6(2)
C10−N2−E1	118.1(2)	115.8(2)	118.2(2)	128.6(2)	128.6(2)	128.9(1)
C1−N1−C5	114.8(2)	117.1(3)	116.8(2)	115.4(3)	115.6(3)	114.9(1)
B1−N1−C1	119.7(2)	119.4(2)	121.6(2)	120.6(3)	117.8(3)	117.3(1)
B1−N1−C5	124.8(2)	121.1(3)	119.8(2)	123.9(3)	115.6(3)	114.1(1)
N2−E1−X1	113.76(8)	113.2(1)	107.22(6)	108.0(2)	100.63(9)	101.62(4)
B1−E1−X2		−		105.6(2)	104.84(9)	98.72(4)
X1−E1−X2	102.37(3)	110.2(1)[a]	116.7(1)[b]	91.2(2)	93.00(5)	90.56(2)

[a] Other C−Sn−C angles 103.1(2) and 112.8(1). [b] Cl1−Sn1−C20 96.0(1), Cl1−Sn1−C21 101.2(1)

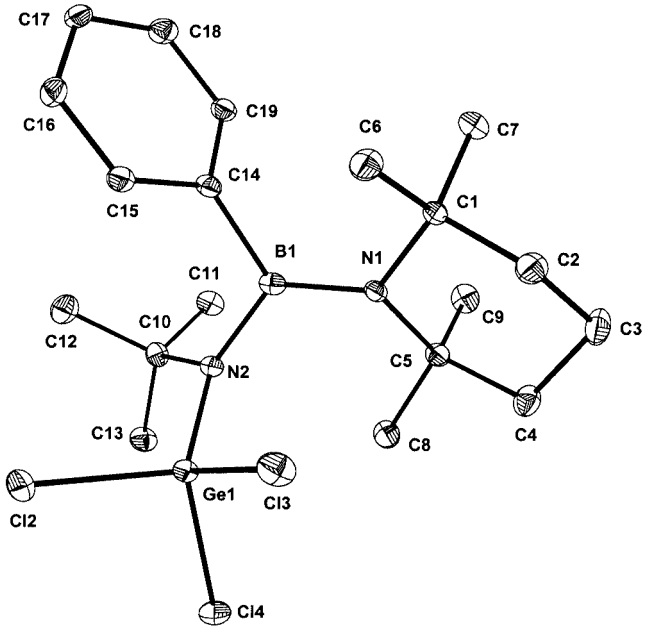

Figure 7. Molecular structure of **11**

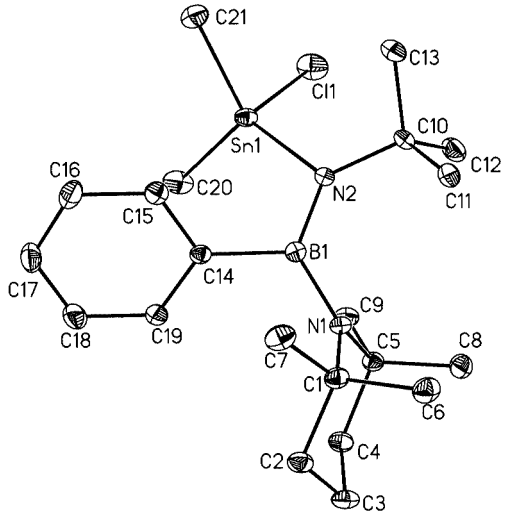

Figure 9. Molecular structure of **13**

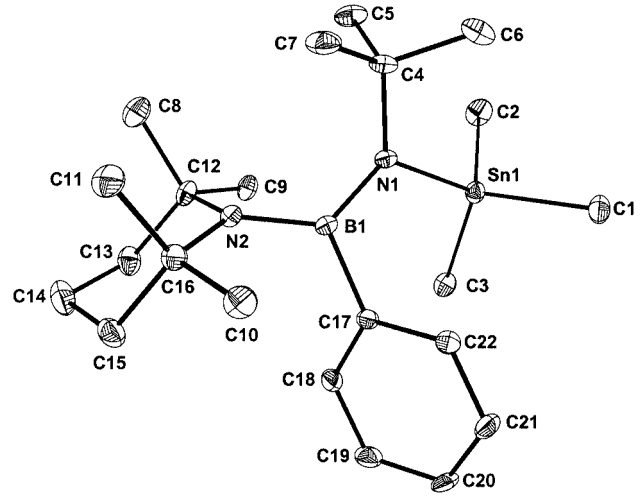

Figure 8. Molecular structure of **12**

ent interplanar angles of 30.9° for N1B1N2/B1N2Sn1 and 117.7° for N1B1N2/C1N1C5. The phenyl group is twisted against the N1B1N2 plane by 43.7°. Thus, the shortening is not a π-bonding effect but is rather due to the stronger electron-withdrawing $SnClMe_2$ substituent. This is also visible in the shorter SnC and SnN bonds in **13** although the differences are small. Notably, the C−Sn−C bond angles in **12** vary from 103.1(2) to 112.8(1)° and for **13** the Cl−Sn−C bond angles are 96.0 and 101.2(1)°, with a wide bond angle of 116.7(1)° for C20−Sn−C21.

Reactions with Halides of Group 15

While **1** reacted with PCl_3 in a 1:1 molar ratio to give an inseparable mixture of products, Ph_2PCl proved unreactive towards **1**. Ph_2PCl is not a strong electrophile, and its behavior corresponds with that of Ph_3GeCl and Ph_3SnCl. In contrast, 1,3,2-benzodioxaphosphorus chloride reacted smoothly with **1** according to Equation (15) to produce the borylated aminophosphane **16**. Its ^{31}P resonance at δ = 163.5 ppm for the tricoordinate P atom lies on the deshielded side for compounds with a PO_2N core.[28] The coupling constant $^2P(^{31}P^{13}C)$ is 23.3 Hz. Its sign, which has not been determined, would allow the determination of the configuration at the P atom. However, the compound is quite clearly noncyclic.

In contrast to PCl_3, both $AsCl_3$ and $SbCl_3$ reacted smoothly in the presence of diethyl ether to give the borylamino-dichloroarsane **17** and the borylamino-dichlorostibane **18**, respectively [Equation (16)]. However, $BiCl_3$ did not react in the nonpolar solvent hexane.

NMR Spectra

NMR spectroscopic data of **16**−**18** are summarized in Table 3. The ^{11}B NMR signals are typical for tricoordinate boron atoms and are slightly deshielded in comparison with the trichlorogermyl and methylstannyl derivatives tmp−BPh−N*t*Bu−EX_2. The protons of the *t*Bu groups are significantly deshielded compared with the compounds listed in Table 1. This seems to be due to the inductive effect of the chlorine atoms that, however, do not affect the protons of the CMe_2 groups, although a particularly large difference is noted for the arsenic compound **17**. In line with this is the deshielding of the ^{13}C nucleus of C10 in **16**, which is also noticeable for **17** and **18**.

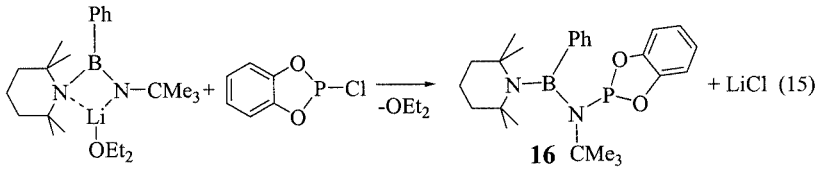

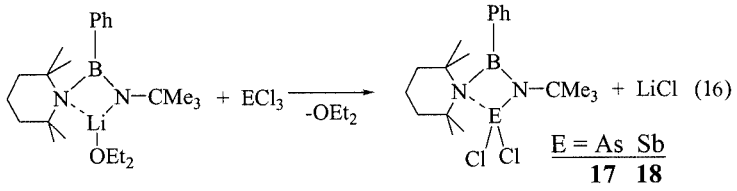

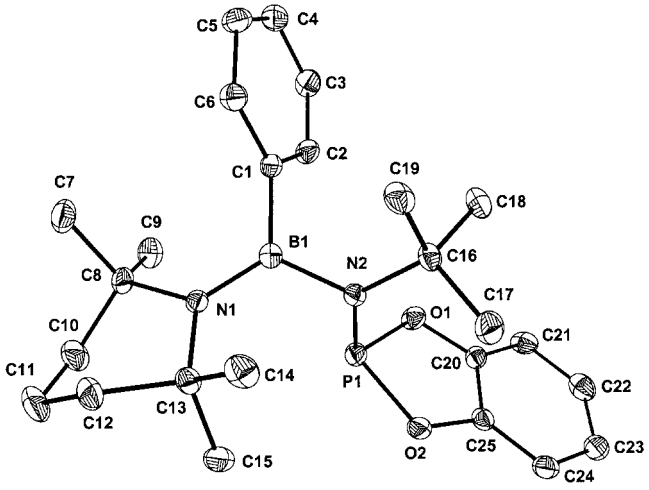

Figure 10. Molecular structure of **16**

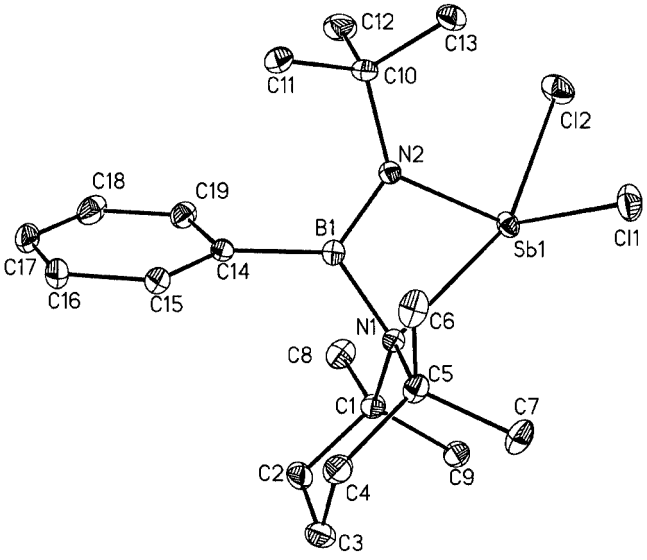

Figure 12. Molecular structure of **18**

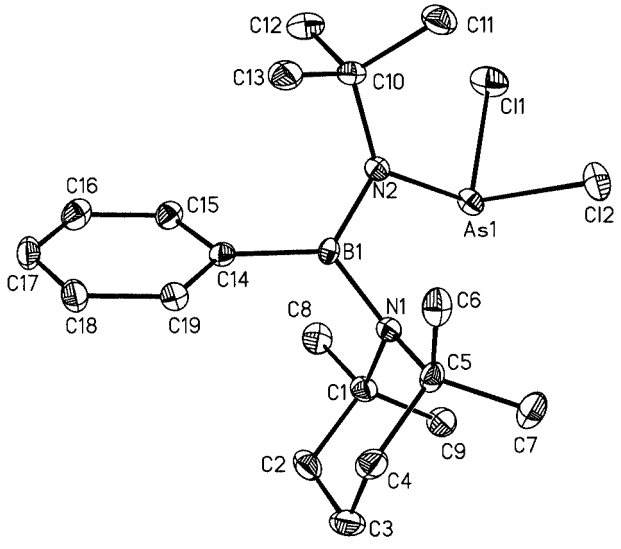

Figure 11. Molecular structure of **17**

Since there are two resonances each for these three compounds for the CMe_2 groups, hindered rotation about the B1–N1 bond is indicated. However, the NMR spectroscopic data are not conclusive as to whether **17** and **18** are cyclic or noncyclic in solution, while the ^{31}P resonance for **16** proves its noncyclic nature in solution. It was, therefore of interest to determine the solid-state structures of these compounds.

Molecular Structures

In analogy to the trichlorogermyl compound **11** there is also a shorter B–N bond in **16** to N1 [1.431(4) Å] than to N2 [1.528(3) Å]. This is due to a more planar arrangement of plane C1–N1–C5 with respect to the plane N1–B–N2 compared with the P1–N2–B1 plane (28.9° and 67.6°, respectively). Thus, there is stronger BN π-bonding to the N1 atom of the tmp unit, which possess not the usual chair conformation but rather the unusual skew conformation. The molecular conformation is, moreover, determined by a sterically most favored conformation; in this the C1N1C5 and C10N2P10 units are practically perpendicular (87.7°). This also allows a sterically favorable arrangement of the *t*Bu and the catecholatophosphorus units by opening the P1–N2–C10 bond angle to 128.5°. Notably, P1 points in the direction of N1 although there is no bonding interaction between these two atoms as the P1···N1 distance is as large as 3.174 Å.

Conversely, the P1−N2 bond is short [1.670(3) Å]. Usually, P−N distances between tricoordinate P atoms and N atom are of the order of 1.80 Å [29]

The arsenic compound **17** shows a *cisoidal* arrangement of the N1B1N2As1 skeleton (Figure 11). B1−N1 π-bonding is excluded as the N1−B1 bond is longer than the B1−N2 bond and, in addition, N1 is not sp^2 as the sum of its bond angles is 349.0°. While the Cl1−As1−Cl2 angle is sharp [93.00(5)°] the N2−As1−Cl bond angle is 104.8(2)° and As1−N2−C10 is as wide as 128.6(2)°. However, the B1−N2−As1 bond angle is only 103.0°, pointing to preformation of a four-membered N1B1N2As1 ring. This, however, seems to be a steric effect exerted by the bulky *t*Bu group, as almost the same situation holds for the antimony compound **18**. Here, the Sb1−N2 bond is 2.072(2) Å and the Sb1−N1 atom distance is 2.539(1) Å. The N1−E and N2−E bond lengths differ by 0.644 Å in **17** and by 0.467 Å in **18**. All bond angles about E1 deviate strongly even for an approximate ψ-trigonal bipyramidal arrangement of atoms about the As and Sb centers, as the N1−As1−Cl1 and N1−Sb1−Cl2 bond angles of 158.4° and 157.6°, respectively, show. No doubt there is a weak E−N1 interaction, which is probably not retained in solution.

Discussion

The results described above demonstrate that **1** is a versatile reagent, leading to noncyclic and cyclic metallated diaminoboranes. The new compounds show structural features that are also present in metallo amidines.[2−8] However, the high steric requirement of the anion of **1** makes it less reactive than several lithium diorganylborylamides $R_2B-NR'Li$.[17,18,31]

Cyclic compounds **2**−**4** are readily accessible, while the cyclic compounds tmp−BX−N*t*Bu−BX_2 (X = Cl, Br) are better obtained by insertion of the BN triple bond of the amino iminoborane tmpB≡N*t*Bu into a boron halogen bond of BX_3.[32] These, like **2**−**4**, exhibit four different B−N bond lengths that depend on the combination of sp^2- and sp^3-type boron and nitrogen atoms; the shortest bonds involve tricoordinate B and N atoms, the longest tetracoordinate B and N atoms. These examples add to the arguments given by Power et al. on the influence of hybridization and multiple bonding in BN systems.[33]

While the catecholatoborane **4** as well as the analogous methyl derivative [1] are cyclic the liquid parent compound tmp−BH−N*t*Bu−Bcat[34] is considered to be noncyclic. This conclusion was based on NMR spectroscopic data. Thus, in contrast to **4**, only one set of ^1H and ^{13}C resonances occurs for the two CMe_2 groups, implying free rotation about the B1−N1 bond, while there are two for **4**. Moreover, even for **4** the B2−N1 bond may break at higher temperatures as it is rather long at 1.741(3) Å, which is close to the longest B−N bond of 1.756 Å found for $B_2Cl_4{\cdot}2NMe_3$.[35]

Halides of Al, Ga, and In react with alkali metal amidinates to give various analogs of the amindinato complexes of these element, all of which have chelate structures with either tetra-, penta- or hexacoordinate metal atoms.[36−39] In this study only one type has been characterized: compounds **6**−**8** are all four-membered chelates with tetracoordinate metal atoms. As expected, the coordinate E1−N1 bond is much longer than the single bond between atoms E1 and N2 (Table 2). Actually, this bond [2.078(2) Å] is longer than in most other amine adducts of $AlR_{3-n}X_n$, for which a range of 1.96−2.04 Å has been reported.[40,41] The Al1−N2 bond in **6** [1.869(2) Å] is longer than the terminal Al−N bonds in $[Al(N{=}CPh_2)_3]_2$ (av. 1.78 Å)[42] and several others,[43] but a better value for comparison is the Al−N bond in $[tmp_2AlF]_2$ [1.832(2) Å] where the fluorine atoms bridge the Al atoms.[20] Its Al−N bonds comprise tetracoordinate Al atoms and a tricoordinate N atom, as observed for **6**. Lesser differences in the two bond lengths are found for cyclic $Me_2Al(N\mathit{t}Bu)_2SMe(N\mathit{t}Bu)$ [1.908(2) and 1.918(2) Å][44] and cyclic $Me_2Al(NC_6H_2\mathit{t}Bu_3)_2P$ [1.974(3) and 1.981(4) Å] although the shorter bonds are longer than in **6**.[45] The same features are observed for **7** and **8**. With **7** the two Ga−N bonds can be compared with those of $[Ga(NMe_2)_3]_2$.[46] In this compound the bridging N atoms show Ga−N bond lengths of 1.964 and 1.974 Å while the Ga−N bonds to the terminal NMe_2 groups are, on average, 2.01 Å. Thus, the Ga1−N1 distance of 2.175(2) Å exceeds those of the bridging NMe_2 groups significantly while the Ga1−N2 bond length of 1.935(2) Å is considerably longer than the Ga−N bond to the terminal NMe_2 groups. The opening of the C−E−C bond angle from **6** to **8** suggests that the weakening of the E1−N1 bond is responsible for this change in structure, and that the In1−N1 bond is the easiest to break. Indeed, in solution this bond opens, as shown by the free rotation of the tmp unit about the B1−N1 bond. Most In−N bond lengths to tetracoordinate In lie in the range 2.196−2.246 Å.[47−50] Consequently, the In1−N1 bond [2.376(2) Å] is weak.

In contrast to the rich chemistry of silylamidines and silylamidinato complexes,[5,51,52] which allows even the synthesis of hexacoordinate Si chelates, no reactions of **1** with either trimethylhalosilanes or triphenylhalosilanes were observed, and even the reaction with $SiCl_4$ was not straightforward − the expected product tmp−BPh−N*t*Bu−$SiCl_3$ could not be isolated. In fact, in the synthesis of silylamidines the products formed are not only dependent on the stoichiometry of the reagents as *trans*-silylation reactions were also observed.[51] From the results obtained, the electrophilic character of element halides clearly plays a decisive role as well as steric factors. While Me_3SiCl and Me_3GeCl do not react with **1**, the more Lewis acidic Me_3SnCl readily did so. However, double substitution of halogen atoms in Me_2SnCl_2 and $SnCl_2$ were unsuccessful. This, we assume, is due to the bulkiness of **13** and **15**.

In line with these observations concerning reactivity, Ph_2PCl does not react with **1** while PCl_3 leads to an inseparable mixture of products. Conversely, the reactions with $AsCl_3$ and $SbCl_3$ produced the well-characterized compounds **17** and **18**. In **17**, the As1−N1 bond is 0.744 Å longer than the As1−N2 bond, indicating only a very

weak interaction. In the analogous compound tmp−BCl−N*t*Bu−$AsCl_2$, As1−N1 is 2.619(4) Å and As1−N2 is 1.869(4) Å.[53] The latter is not significantly shorter than in **17** [1.872(3) Å]. As−N bonds to tricoordinate As and tricoordinate N atoms span the range 1.79−1.95 Å.[53−55] The compound closest in structure to **17** is the cyclic $ClAs(NPPh_3)_2SbCl_4$,[53] with As−N bond lengths of 1.843 and 1.946 Å; compound **19** is even more closely related.[54] The difference in Sb−N bonds lengths in **18** is 0.467 Å, and in tmp−BCl−N*t*Bu−$SbCl_2$ 0.471 Å.[55] Comparable Sb−N bond lengths in $Cl_2Sb(NSiMe_3)_2CPh$ are 3.262 and 2.122 Å [56] or 4.144 and 2.097 Å for $Cl_2Sb(NSMe_2NSiMe_3)SbCl_2$.[57] Therefore, these latter two compounds exhibit much weaker Sb−N interactions than Sb1−N1 in **18**.

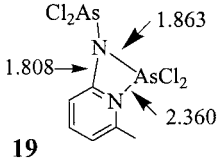

19

In conclusion, there are many analogies between the aminoborylamides and amidates, although **1** seems to be not as efficient a reagent as $R_2NCR-NR$ anions. This, however, is due to the large steric requirements of the anion of **1**. Thus, alkali metal salts with an anion $R_2N-BR'-NR''^-$ with R, R′, R″ = Me or R, R′ = Me and R″ = *i*Pr will be closer in reactivity to smaller amidates. However, *N*-metallated amino-, diamino- and triaminoboranes undoubtedly offer a wide new field for research and application.

Experimental Section

General Remarks: All experiments were conducted under anhydrous conditions using the Schlenk technique. Element halides or methyl element halides were commercial products of high quality. Compound **1** was prepared as described previously[1] or by the alternative procedure described below.

Elemental analyses were performed at the department's microanalytical laboratory. NMR: Bruker ACP-200 (^{7}Li, ^{11}B, ^{31}P, ^{119}Sn) or Jeol EX 400 (^{1}H, ^{13}C, ^{19}F); internal standards: C_6D_6, $CDCl_3$; external standards (1 M aqueous LiCl, H_3PO_4, $SnMe_4$) for all other nuclei. Mass spectra: VARIAN Atlas CH7; the mass numbers given refer to the most abundant isotope, and mass, relative intensity and assignment are reported. X-ray diffraction: Siemens P4 four circle diffractometer with a CCD area detector and LT2 device, Mo-K_α radiation, graphite monochromator. Data collection was performed with the programs implemented in SMART.[59]

(*tert*-Butylamino)[phenyl(2,2,6,6-tetramethylpiperidino)boryl]-lithium−Diethyl Ether (1): A solution of $tmpBCl_2$ (3.8 mL, 18 mmol) in hexane (20 mL) was added to a suspension of $LiHNCMe_3$ (1.44 g, 18.0 mmol) in hexane (30 mL). After stirring for 1 h the resultant precipitate was filtered off. All volatile material from the filtrate was then removed by distillation and the resultant oily residue of tmp−BCl−$NHCMe_3$ subjected to vacuum distillation (b.p. of 63 °C/0.001 Torr). Some $tmpB(NHCMe_3)_2$ was also obtained (higher boiling fraction). A 2 M solution of LiPh in cyclohexane/diethyl ether (8:2, 10.0 mL) was added dropwise while stirring to this bis(amino)chloroborane dissolved in hexane (100 mL). The resulting precipitate (LiCl) was filtered off, and the solvents were removed from the filtrate in vacuo. The so-obtained residue was then dissolved in hexane (30 mL) and the solution cooled to −20 °C. Within a few days colorless crystals separated. Yield: 3.4 g of **1** (95%). For further reactions, the suspension containing LiCl can be used directly.

General Procedure: A solution of the element halide compound was added to a freshly prepared and stirred solution of **1** in hexane at −78 °C. The insoluble material that formed in most of the reactions was removed by filtration (glass frit), and the solvents from the filtrate in vacuo. The residue was then crystallized from a suitable solvent.

2-*tert*-Butyl-5,5,9,9-tetramethyl-1-phenyl-2-aza-4-azonia-1-bora-3-borataspiro[3.5]nonane (2): A solution of BH_3·THF (1.77 mL, 3.4 M, 6.0 mmol) diluted with THF (100 mL) was added to **1** (3.0 mmol) in hexane (25 mL) at −78 °C. After warming to ambient temperature the ^{11}B NMR spectrum (^{1}H coupled) of the turbid solution shows a quintuplet at δ = −40.7 ppm ($LiBH_4$), a singlet at δ = 32.7 ppm (BPh), and a triplet at δ = −4.4 ppm (BH_2). All solvents were then removed and the residue extracted with hexane (about 25 mL) to leave behind white $LiBH_4$. The filtrate was subsequently reduced to about 15 mL. At −20 °C colorless crystals of **2** separated within a few days. Yield: 0.73 g (79%); m.p. 113 °C. $C_{19}H_{34}B_2N_2$ (312.09): calcd. C 73.29, H 10.61, N 9.00; found C 72.04, H 11.21, N 8.66. MS: (70 eV): *m*/*z* (%) = 312 (100) [M^+], 297 (62) [M^+ − Me], 255 (18) [M^+ − Bu], 240 (13) [M^+ − Me − Bu], 227 (43) [M^+ − H_2B − NBu], 187 (46) [M^+ − 125], 171 (35) [M^+ − tmpH], 144 (47) [M^+ − $tmpBH_2$ − Me], 126 (78) [tmp − Me^+].

2-*tert*-Butyl-3,3-difluoro-5,5,9,9-tetramethyl-1-phenyl-2-aza-4-azonia-3-borataspiro[3.5]nonane (3): A solution of BF_3·OEt_2 (0.75 mL, 6.0 mmol) in diethyl ether (10 mL) was slowly added, with stirring, to a solution of **1** (3.0 mmol) in hexane (30 mL). The solution showed at ambient temperature two ^{11}B singlet signals of almost equal intensity at 35.7 (BPh) and δ = 1.6 ppm ($LiBF_4$) (broad) and a triplet at δ = 4.8 ppm (BF_2). All volatile components were then removed in vacuo and the residue extracted with several portions of hexane. Subsequently, the insoluble $LiBF_4$ was removed from the last portion of the extracting hexane solution. The combined filtrates were then reduced to about 15 mL and kept at −20 °C. Within a few days, clear crystals of **3** separated. Yield: 0.7 g (72%), m.p. 121 °C. $C_{19}H_{32}B_2F_2N_2$ (348.08): calcd. C 65.50, H 9.19, N 8.04; found C 67.41, H 9.14, N 7.78. MS (70 eV): *m*/*z* (%) = 348 (4.5) [M^+], 333 (100) [M^+ − Me], 277 (82) [M^+ − Bu], 228 (15) [$tmpBPh^+$], 222 (16) [$tmpBNtBu^+$], 126 (23) [tmp − Me^+].

3-(Benzodioxo)-2-*tert*-butyl-5,5,9,9-tetramethyl-1-phenyl-2-aza-4-azonia-1-bora-3-borataspiro[3.5]nonane (4): A solution of *B*-chlorocatecholborane (0.46 g, 3.0 mmol) in diethyl ether (10 mL) was added at room temperature to a hexane solution of **1** (3.0 mmol). A white precipitate formed immediately. After stirring overnight the precipitate was separated by filtration and the filtrate reduced to 15 mL in vacuo. At −78 °C colorless crystals of **4** formed. Yield: 0.92 g (76%), m.p. 185 °C. $C_{25}H_{36}B_2N_2O_2$ (417.6): calcd. C 71.80, H 8.68, N 6.70; found C 71.83, H 8.97, N 6.69. MS (40 °C, 70 eV): *m*/*z* = 417 [M^+], 403 [M^+ − Me], 347 [M^+ − Me − Bu], 318 [$PhBNBu^+$], 277 [M^+ − tmp], 222 [$tmpBNBu^+$], m* = 298.8.

(2,2,6,6-Tetramethylpiperidine)lithium *tert*-Butyl[phenyl(2,2,6,6-tetramethylpiperidino)boryl]amide (6): A solution of **1** (3.0 mmol) in hexane (25 mL) was allowed to react at ambient temperature with

a solution of tmp_2AlCl (3.0 mmol, 12.6 mL of a 0.238 M solution in hexane). The turbid mixture was then maintained at reflux for 1 d; 50% of **1** had reacted to a new compounds with $\delta^{11}B = 35.7$ ppm. Additional heating afforded no change in the ^{11}B NMR spectrum. The precipitate that had formed was filtered off. The yellow filtrate was then kept at −20 °C, providing a small amount of crystals of **6** that showed an ^{11}B NMR signal at δ = 35.5 ppm but no ^{27}Al NMR signal; m.p. 210 °C (dec.). $C_{28}H_{51}BLiN_3$ (447.47): calcd. C 75.16, H 11.49, N 9.39; found C 72.93, H 10.65, N 8.98. MS (70 eV): *m*/*z* (%) = 299 (100) [M^+ − tmpH − Li], 284 (100) [299 − Me^+], 243 (12) [299 − Bu^+], 126 (100) [tmp − Me^+].

2-*tert*-Butyl-3,3,5,5,9,9-hexamethyl-1-phenyl-2-aza-4-azonia-1-bora-3-aluminataspiro[3.5]nonane (7): A 1 M solution of Me_2AlCl in hexane (3 mL) was added to a suspension of **1** with LiCl (3.0 mmol **1** in 30 mL of hexane/diethyl ether) at room temperature. After stirring for 1 h the insoluble material was filtered off and the so-obtained colorless solution reduced to 15 mL. At −20 °C, colorless, moisture and air-sensitive crystals separated. Yield: 0.92 g of **7** (86%), m.p. 160 °C. $C_{21}H_{38}AlBN_2$ (356.32): calcd. C 70.72, H 10.66, N 7.88; found C 63.81, H 9.17, N 6.70. ^1H NMR (C_6D_6): δ = −0.06 (s, 6 H, $AlMe_2$) ppm. ^{13}C NMR ((C_6D_6): δ = 0.24 (br., $AlMe_2$) ppm. ^{27}Al NMR (C_6D_6): δ = 164, ($h_{1/2}$ = 1800 Hz) ppm. MS (70 eV): *m*/*z* (%) = 356 (8.5) [M^+], 341 (100) [M^+ − Me], 300 (21.5) [M^+ − Bu], 284 (100) [M^+ − Me − Bu], 269 (64) [284 − Me^+], 256 (32) [Me_2NBu^+], 228 (36.5) [tmpBPh$^+$], 216 (100) [M^+ − tmp], 183 (100) [tmpAlMe$^+$], 159 (100) [PhBNBu$^+$].

2-*tert*-Butyl-3,3,5,5,9,9-hexamethyl-1-phenyl-2-aza-4-azonia-1-bora-3-gallataspiro[3.5]nonane (8): Prepared in analogy to **7** by using Me_2GaCl (0.45 g, 3.0 mmol) dissolved in hexane (30 mL) to furnish very moisture- and air-sensitive crystals of **8**. Yield: 1.05 g (88%). $C_{21}H_{38}BGaN_2$ (399.06): calcd. C 63.1, H 9.52, N 7.02; found C 58.18, H 8.43, N 6.29. ^1H NMR (C_6D_6): δ = 0.32 (s, GaMe ppm.^{13}C NMR (C_6D_6): δ = 1.13 ($GaMe_2$) ppm. MS (70 eV): *m*/*z* (%) = 399 (0.5) [M^+], 384 (43) [M^+ − Me], 297 (9.5) [$GaMe_2^+$?], 224 (42) [tmpGaMe$^+$], 126 (11.5) [tmp − Me^+].

2-*tert*-Butyl-3,3,5,5,9,9-hexamethyl-1-phenyl-2-aza-4-azonia-1-bora-3-indataspiro[3.5]nonane (9): Prepared in analogy to **7** by using Me_2InCl (0.54 g, 3.0 mmol) dissolved in hexane (20 mL), with workup after stirring for 5 h. The filtrate was then reduced to ca. 20 mL. Crystals of **9** separated from the solution at −78 °C. Yield: 0.90 g (68%), m.p. > 200 °C. $C_{21}H_{38}BInN_2$ (444.16): calcd. C 56.74, H 8.56, N 6.30; found C 51.04, H 7.96, N 5.78. ^1H NMR (C_6D_6): δ = 0.06 (s, $InMe_2$) ppm. ^{13}C NMR ($CDCl_3$): δ = 1.0 ($InMe_2$) ppm.

Insufficient protection against air for **7**−**9** is responsible for the large deviation between calculated and found values in the elemental analysis.

[(*tert*-Butyl)(trimethylsilyl)amino](phenyl)(2,2,6,6-tetramethylpiperidino)borane (10): Li(tmp) (0.87 g, 5.9 mmol) was suspended in hexane (30 mL). After cooling the suspension to −78 °C, a solution of $PhBCl_2$ (0.78 mL, 5.9 mmol) in hexane (5 mL) was added with stirring. At room temperature only a single signal at $\delta^{11}B$ = 41.8 ppm was present, showing the complete conversion of $PhBCl_2$. The solid was filtered off and the filtrate treated with a freshly prepared solution of Li*N*t*Bu*($SiMe_3$) (5.9 mmol) in hexane (20 mL). The mixture was then kept under reflux for 5 d. Three ^{11}B NMR signals, at δ = 34.2 (60%), 23.4 (15%) and at 28.0 (25%) ppm, were detected, the first of which corresponds to **10**. In addition, three ^{27}Si NMR signals were found at δ = 9.1 (main signal), 17.6 and δ = 8.0 ppm. After removal of the hexane in vacuo the residue was treated with hexane (10 mL), the solid was removed by filtration and the so-obtained yellow solution kept at −20 °C. No crystals separated. Also, distillation did not allow **10** to be separated from the by-products.

[(*tert*-Butyl)(trichlorogermyl)amino](phenyl)(2,2,6,6-tetramethylpiperidino)borane (11): The solvent from a freshly prepared solution of **1** (1.77 mmol) in hexane (30 mL) was removed and the residue dissolved in diethyl ether (40 mL). $GeCl_4$ (0.3 mL) was then added to this solution, and the resultant suspension kept at reflux for 2 h. Since no complete conversion was noted the mixture was maintained at reflux for 5 days, after which only a single ^{11}B NMR signal was seen. The ether was then removed and the resultant oily residue treated with hexane (40 mL). On reducing the filtrate's volume to about 50%, crystals of **11** separated at −20 °C. Yield: 0.63 g (75%), m.p. 205 °C. $C_{19}H_{32}BCl_3GeN_2$ (478.22): calcd. C 47.68, H 6.69, N 5.85, Cl 22.24; found C 47.45, H 6.73, N 5.75, Cl 20.91.

[(*tert*-Butyl)(trimethylstannyl)amino](phenyl)(2,2,6,6-tetramethylpiperidino)borane (12): Prepared in analogy to **11** from **1** in hexane (3.0 mmol, 20 mL) and Me_3SnCl (0.76 g, 2.8 mmol) in hexane (15 mL). The suspension was then stirred for 2 days. Although only the ^{11}B NMR signal of **12** (δ = 39.8 ppm) was noted, the first crystals that separated from the filtrate at −20 °C proved to be Me_3SnCl. These were removed and the filtrate kept at −78 °C to afford crystals of **12**. Yield: 0.97 g (70%), m.p. 98 °C. $C_{22}H_{41}BN_2Sn$ (464.24): calcd. C 57.01, H 8.85, N 6.05; found C 54.80, H 8.68, N 5.68. ^1H NMR (C_6D_6): δ = 0.08 [t, $^2J(^{119}Sn^1H)$ = 56.3 Hz, 9 H] ppm. ^{13}C NMR (C_6D_6): δ = 1.4 [$^1J(^{119}Sn^{13}C)$ = 395.1 Hz] ppm. ^{119}Sn NMR (C_6D_6): δ = 17.9 ppm. MS (70 eV): *m*/*z* (%) = 464 (22) [M^+], 449 (100) [M^+ − Me], 324 (100) [M^+ − tmp], 165 (100) [$SnMe_3^+$].

[(*tert*-Butyl)(chlorodimethylstannyl)amino](phenyl)(2,2,6,6-tetramethylpiperidino)borane (13): A solution of Me_2SnCl_2 (0.44 g, 2.0 mmol) dissolved in boiling hexane (50 mL) was added to freshly prepared **1** (2.0 mmol) in hexane (30 mL) kept at −78 °C. The resulting suspension showed, at ambient temperature, only a single ^{11}B NMR signal at δ = 39.4 ppm. The filtrate was then reduced to 20 mL, and on cooling to −20 °C crystals of **13** separated. Yield: 0.71 g (73%), m.p. 145 °C (dec.). $C_{21}H_{38}BClN_2Sn$ (483.48): calcd. C 52.12, H 7.86, N 5.79; found C 45.67, H 7.51, N 5.74. ^1H NMR (C_6D_6): δ = 0.02 [d, $^2J(^{119}Sn^1H)$ = 52 Hz, 6 H, $SnMe_2$] ppm. ^{13}C NMR (C_6D_6): δ = −2.6 [$^1J(^{119}Sn^{13}C)$ = 390 Hz] ppm. ^{119}Sn NMR (C_6D_6): δ = 93.1 ppm.

Reaction of Me_2SnCl_2 with 1 in a 1:2: Ratio: In analogy to **13**, Me_2SnCl_2 (2.0 mmol) in hexane (50 mL) was reacted with **1** [4.0 mmol in hexane (40 mL)] at −78 °C. The ^{11}B NMR spectrum of the suspension showed, at ambient temperature, a signal at δ = 39.2 ppm in addition to that of the starting material. After 3 days, additional signals appeared at δ = 48.3 and δ = 5.4 ppm. A ^{119}Sn NMR spectrum revealed a signal at δ = 98.3 ppm, corresponding to $tmpMe_2SnCl$, while the ^{11}B NMR signal at δ = 39.2 ppm is typical for (tBuNBPh)$_2$.[23]

{(*tert*-Butyl)[chlorostannyl(II)]amino}(phenyl)(2,2,6,6-tetramethylpiperidino)borane (15): $SnCl_2$ (0.38 g, 2.0 mmol) was dissolved in THF (30 mL) and treated at 0 °C with a freshly prepared solution of **1** (4.0 mmol) in hexane (40 mL). A suspension formed, and the ^{11}B NMR spectrum shows a 50% conversion of **1**. On further stirring, no change was observed. After filtration and removal of solvent in vacuo a yellow oil remained that was dissolved in hexane (20 mL). At −20 °C compound **15** separated as a slightly yellow solid that is soluble in benzene, tetrahydrofuran or chloroform. No single crystals separated from these solutions. $C_{19}H_{32}BClN_2Sn$ (454.14): calcd. C 50.33, H 7.11, N 6.18; found C 48.75, H 7.05, N 5.51. MS (70 eV): *m*/*z* (%) = 454 (9) [M^+], 439 (25) [M^+ − Me],

419 (9) [M^+ − Cl], 301 (60) [M^+ − MeSnCl], 278 (100) [M^+ − Cl − tmp], 126 (77)) [tmp − Me^+].

{(*tert*-Butyl)[(phenyl)(2,2,6,6-tetramethylpiperidino)boryl]amino}-1,3,2-benzodioxaphosphane (16): A solution of benzodioxaphosphorus chloride (0.35 g, 2.0 mmol) in toluene (20 mL) was added to a solution of **1** (2.0 mmol) in hexane (40 mL) with stirring to afford a white precipitate that dissolved on prolonged stirring. After 3 days, the reaction was complete (^{11}B NMR signal at δ = 41.1 ppm). Following removal of the solvents the resultant oily, semi-solid residue was treated with toluene (30 mL) and the insoluble material filtered off. From the filtrate, crystals of **16** separated at −20 °C. Yield: 0.59 g (67%), m.p. 177 °C. $C_{26}H_{36}BN_2O_2P$ (438.36): calcd. C 68.53, H 8.23, N 6.39; found C 64.88, H 8.32, N 6.30. ^{1}H NMR (C_6D_6): δ = 6.69 [dd, $^3J(^1H^1H)$ = 5.76, $^4J(^1H^1H)$ = 3.4 Hz], 6.95 [dd, $^3J(^1H^1H)$ = 5.76, $^4J(^1H^1H)$ = 3.2 Hz, cat H], 7.17, 7.18, 7.71

Table 5. Crystallographic data and data related to data collection and structure refinement

Compound	**2**	**3**	**4**	**6**	**7**	**8**
Chem. formula	$C_{19}H_{35}N_2B_2$	$C_{19}H_{33}N_2B_2F_2$	$C_{25}H_{36}N_2B_2O_2$	$C_{28}H_{51}N_3BLi$	$C_{21}H_{38}N_2AlB$	$C_{21}H_{38}N_2BGa$
Form. wght.	312.09	348.08	418.18	447.47	356.32	399.06
Cryst. size [mm]	0.30 x0.30 x0.40	0.15 x0.20 x0.20	0.5x0.5x0.6	0.2x0.3x0.4	0.09 x0.20 x0.30	0.30 x0.30 x0.40
Cryst. system	Orthorhombic	Orthorhombic	Monoclinic	Triclinic	Monoclinic	Monoclinic
Space group	Pnma	Pnma	P2(1)/n	P-1	P2(1)/c	P2(1)/c
a, [Å]	18.8488(4)	18.8134(2)	9.296	10.3038(7)	11.9770(5)	12.0288(3)
b, [Å]	11.3274(2)	11.400(1)	14.0167(2)	10.9388(8)	13.0568(7)	13.0359(1)
c, [Å]	8.9697(2)	8.9891(2)	18.1577(2)	14.6358(11)	13.9489(7)	13.9379(1)
α, [°]	90	90	90	70.850(1)	90	90
ß, [°]	90	90	93.505(1)	69.601(2)	92.143(2)	92.309(1)
γ, [°]	90	90	90	71.577(1)	90	90
V, [Å^3]	1915.10(7)	1927.88(5)	2361.51(4)	1422.3(2)	2179.82(18)	2183.78(6)
Z	4	8	4	2	4	4
ρ(calcd.), [Mg/m^3]	1.079	1.199	1.176	1.045	1.086	1.214
μ [mm^{-1}]	0.061	0.082	0.072	0.059	0.099	1.266
F(000)	684	752	904	496	784	856
Index range	-21<h<23	-25<h<21	-10<h<10	-11<h<14	-15<h<8	-11<h<16
	-14<k<14	-14<k<14	-15<k<13	-14<k<14	-15<k<16	-16<k<16
	-11<l<11	-11<ll<11	-21<l<21	-18<l<18	-17<l<17	-17<l<17
2 θ [°]	58.00	57.96	49.42	58.38	57.66	58.08
Temp, [K]	193	193	193	193	193	193
Refl. collected	10517	10715	11135	8389	12242	12131
Refl. unique	2115	2173	3661	4561	3703	3954
Refl. observed (4σ)	1730	1531	2795	3130	2455	3486
R (int.)	0.0403	0.0358	0.0400	0.0269	0.0526	0.0165
No. variables	127	141	280	302	226	227
Weight. Scheme x/y	0.0617/0.9314	0.0325/1.5867	0.0457/0-5923	0.0657/0.8623	0.0789/2.395	0.100/0
GOOF	1.265	1.024	1.156	1.101	1.014	1.036
Final R (4σ)	0.0665	0.0524	0.0465	0.0688	0.0637	0.0353
Final wR2	0.1650	0.1329	0.1131	0.1589	0.1470	0.0939
Larg. res. peak [e/Å^3]	0.543	0.334	0.274	0.279	0.396	0.675

Compound	**9**	**11**	**12**	**13**	**16**
Chem. formula	$C_{21}H_{38}BInN_2$	$C_{19}H_{32}BCl_3GeN_2$	$C_{22}H_{41}BN_2Sn$	$C_{21}H_{38}BClN_2Sn$	$C_{25}H_{36}BN_2O_2P$
Form. wght.	44.16	478.22	463.07	483.48	438.34
Cryst. size [mm]	0.2x0.3x0.3	0.2 x0.2 x0.3	0.1 x0.3 x0.3	0.20 x0.20 x0.30	0.10 x0.15 x0.20
Cryst. system	triclinic	Monoclinic	Triclinic	Monoclinic	Monoclinic
Space group	P-1	P2(1)/n	P-1	C2/c	P2(1)
a, [Å]	8.4799(1)	11.0513(6)	7.6774(1)	27.323(4)	12.765(5)
b, [Å]	10.7491(2)	14.7340(8)	9.9774(2)	9.1863(12)	7.837(3)
c, [Å]	12.5190(1)	13.9329(8)	16.7750(2)	19.328(3)	13.466(6)
α, [°]	97.582(1)	90	95.763(1)	90	90
ß, [°]	97.194(1)	106.0850(1	97.662(1)	106.896(2)	115.268(6)
γ [°]	93.232(1)	90	111.113(1)	90.	90
V, [Å^3]	1119.15(3)	2179.9(2)	1172.60(3)	4641.9(11)	1218.3(8)
Z	2	4	2	8	2
ρ(calcd.), [Mg/m^3]	1.318	1.457	1.312	1.384	1.195
μ [mm^{-1}]	1.062	1.780	1.097	1.223	0.136
F(000)	464	992	484	2000	472
Index range	-10<h<10	-14<h<14	-9<h<9	-33<h<31	-16<h<16
	-13<k<13	-19<k<16	-8<k<13	-11<k<11	-10<k<9
	-15<l<15	-17<l<17	-21<l<21	-24<l<24	-16<l<16
2 θ [°]	58.48	58.54	57.36	56.44	58.14
Temp, [K]	173(2)	183(2)	193	193	188(2)
Refl. collected	6735	12416	6804	11634	7003
Refl. unique	3596	4297	3697	4177	4680
Refl. observed (4σ)	3363	3278	3371	3549	3394
R (int.)	0.0108	0.0731	0.0161	0.0245	0.0319
No. variables	251	242	235	235	281
Weight scheme[1] x/y	0.0o789	0.35950.057/0.00	0.0216/6.3872	0.0532/0.4504	0.0643/0.1977
GOOF	1.148	1.045	1.097	1.145	1.017
Final R (4σ)	0.0224	0.0397	0.0263	0.0308	0.0602
Final wR2	0.619	0.0869	0.0677	0.0820	0.1288
Larg. res. peak [e/Å^3]	0.434	0.435	0.353	0.982	0.182

Table 5 *(continued)*

Compound	**17**	**18**
Chem. formula	$C_{19}H_{32}AsBCl_2N_2$	$C_{19}H_{32}B\,Cl_2N_2Sb$
Form. wght.	445.10	491.93
Cryst. size [mm]	0.20 x0.20 x0.30	0.1 x0.2 x0.2
Cryst. system	Monoclinic	Monoclinic
Space group	P2(1)/c	P2(1)/c
a, [Å]	11.3035(6)	11.599(2)
b, [Å]	13.8516(8)	13.980(3)
c, [Å]	13.5671(7)	13.244(3)
α, [°]	90	90
β, [°]	90.903(1)	93.280(9)
γ, [°]	90	90
V, [Å3]	2124.0(2)	2144.1(8)
Z	4	4
ρ(calcd.), [Mg/m3]	1.392	1.524
μ [mm-1]	1.857	1.541
F(000)	928	1000
Index range	-7 <h<14	-15<h<15
	-16<k<16	-18<k<18
	-16<l<16	-17<l<17
2 θ [°]	57.84	57.38
Temp, [K]	193	193
Refl. collected	12031	31857
Refl. unique	3426	5318
Refl. observed (4σ)	2866	4291
R (int.)	0.0728	0.0316
No. variables	233	226
Weight scheme[1] x/y	0.1133/4.9651	0.0251/0.3618
GOOF	0.717	1.027
Final R (4σ)	0.0436	0.0219
Final wR2	0.1088	0.0497
Larg. res. peak [e/Å3]	0.537	0.397

[1] $w^{-1} = \sigma^2F_o^2 + (xP^2 + yP)$; $P = (F_o^2 + 2F_c^2)/3$.

(Ph) ppm. ^{13}C NMR (C_6D_6): δ = 112.3, 122.0 (cat C), 126.8, 128.9, 136.0 (Ph) ppm. ^{31}P NMR (C_6D_6): δ = 163.5 ppm.

{*tert*-Butyl[phenyl(2,2,6,6-tetramethylpiperidino)boryl]-amino}dichloroarsane (17): A solution of $AsCl_3$ (0.17 mL, 2.0 mmol) in hexane (10 mL) was added to a hexane solution of **1** (2.0 mmol in 30 mL). The mixture turned black and on continued stirring became a brownish suspension. After 3 h a ^{11}B NMR signal at δ = 41.3 ppm was detected. The solid was then removed and the yellow solution reduced to about 20 mL. At −20 °C an amorphous solid separated that was crystallized from hexane at ambient temperature. Yield: 0.58 g of **17** (65%), m.p. > 200 °C. $C_{19}H_{32}AsBCl_2N_2$ (445.10): calcd. C 51.22, H 7.19, N 6.29, Cl 15.93; found C 51.15, H 7.46, N 6.29, Cl 15.62.

{*tert*-Butyl[phenyl(2,2,6,6-tetramethylpiperidino)boryl]amino}-dichlorostibane (18): This was prepared from $SbCl_3$ (0.46 g, 2.0 mmol) and **1** (2.0 mmol) in hexane (30 mL). After 3 h the insoluble material was removed by filtration, and on cooling the filtrate (−20 °C) crystals of **18** separated. These crystals are highly sensitive to moisture. Yield: 0.65 g (66%), m.p. 144 °C. $C_{19}H_{32}N_2BCl_2Sb$ (491.93): calcd. C 46.35, H 6.50, N 5.69; found C 45.32, H 6.42, N 5.38. MS (79 eV): *m*/*z* (%) = 473 (25) [M^+ − Me], 456 (7) [M^+ − Cl], 332 (15) [tmpSbCl$_2^+$], 318 (33) [332 − Me^+].

X-ray Structure Determinations: Single crystals were covered with a polyfluoro ether oil and a specimen selected and mounted on the tip of a glass fiber. After cooling the crystal on the goniometer head to −80 °C with an LT2 device, the unit cell was determined from reflection collected on a total of 60 frames at five different settings of the ω and χ circles. Data collection was performed in the hemisphere mode (1264 frames). The program SAINT[59] was used for data reduction, and an absorption correction was applied using SADABS.[60] The structures were solved by direct methods (heavy atom methods for the Sb compound) using SHELX97.[61] This program was also applied for structure refinement. Non-hydrogen atoms were refined with anisotropic description. Most hydrogen atoms were visible after anisotropic refinement, but were placed in calculated positions and included in the refinement by applying a riding model. Data related to crystallography, data reduction and refinement are summarized in Table 5. CCDC-226743 to -226753 and -231319 (**9**) contain the supplementary crystallographic data for this paper. These data can be obtained free of charge at www.ccdc.cam.ac.uk/conts/retrieving.html [or from the Cambridge Crystallographic Data Centre, 12 Union Road, Cambridge CB2 1EZ, UK; Fax: +44-1223-336-033; E-mail: deposit@ccdc.cam.ac.uk].

[1] U. Braun, B. Böck, T. Habereder, H. Nöth, M. Schwartz, S. Weber, U. Wietelmann, *Eur. J. Inorg. Chem.*, in print.
[2] A. R. Sanger, *Inorg. Chem. Lett.* **1973**, *9*, 351−354.
[3] R. T. Boeré, R. T. Oakley, R. W. Reed, *J. Organomet. Chem.* **1987**, *331*, 161−167.
[4] K. Dehnicke, C. Ehrgeizinger, E. Hartmann, A. Binn, *J. Organomet. Chem.* **1988**, *352*, 161−167.
[5] K. Dehnicke, *Chemiker-Ztg.* **1990**, *114*, 295−304.
[6] G. Ehrgeizinger, F. Weller, K. Dehnicke, *Z. Naturforsch., Teil B* **1988**, *43*, 1119−1124.
[7] J. Barker, N. C. Blacker, P. R. Phillips, N. W. Alcock, W. Errington, M. G. H. Wallbridge, *J. Chem. Soc., Dalton Trans.* **1996**, 431−437.
[8] H. Roesky, B. Meller, M. Noltemeyer, H.-G. Schmidt, U. Scholz, G. M. Sheldrick, *Chem. Ber.* **1988**, *121*, 1403−1406.
[9] H. Chen, R. A. Bartlett, M. M. Olmstead, P. P. Power, S. C. Shoner, *J. Am. Chem. Soc.* **1990**, *112*, 1048−1055.
[10] R. A. Bartlett, H. Chen, H. V. R. Dias, M. M. Olmstead, P. P. Power, *J. Am. Chem. Soc.* **1988**, *110*, 446−449.
[11] R. A. Bartlett, X. Feng, M. M. Olmstead, P. P. Power, K. J. Weese, *J. Am. Chem. Soc.* **1988**, *110*, 4851−4854.
[12] B. Wrackmeyer, B. Schwarz, J. Weidinger, W. Milius, *Z. Naturforsch., Teil B* **1997**, *5*, 431−433.
[13] T. Seifert, W. Storch, M. Vosteen, *Eur. J. Inorg. Chem.* **1998**, 1343−1349.
[14] M. J. S. Dewar, P. M. Maitlis, *J. Am. Chem. Soc.* **1961**, *83*, 187−193.
[15] R. J. Wagner, J. L. Bradford, *Inorg. Chem.* **1962**, *1*, 99−106.
[16] H. Nöth, H. Vahrenkamp, *J. Organomet. Chem.* **1969**, *16*, 357−369.
[17] D. Fest, C. D. Habben, A. Meller, G. M. Sheldrick, D. Stalke, F. Pauer, *Chem. Ber.* **1990**, *123*, 703−706.
[18] C. D. Habben, A. Heine, G. M. Sheldrick, D. Stalke, *Z. Naturforsch., Teil B* **1992**, *47*, 1367−1369.
[19] Most likely the first reaction product is [tmp−PhB−N*t*BuBH$_3$]Li which will react with BH$_3$·THF to give LiBH$_4$ and *cyclo*-tmp−BPh−N*t*Bu−BH$_2$ (**2**).
[20] I. Krossing, H. Nöth, L. C. Tacke, M. Schmidt-Amelunxen, H. Schwenk-Kircher, *Chem. Ber./Receuil* **1997**, *130*, 1047−1052.
[21] The ^{27}Al resonance of tmp$_2$AlBr·OEt$_2$ was observed at δ = 125 ppm. I. Krossing, Ph.D. Thesis, University of Munich, **1997**.
[22] For [tmpAl(OEt)Cl]$_2$ a ^{27}Al resonance at δ = 89 ppm was observed. C. Tacke, PhD Thesis, University of Munich, **1994**.
[23] H. Nöth, B. Wrackmeyer, *Nuclear Magnetic Resonance Spectroscopy of Boron Compounds*, NMR Basic Principles and Progress (Eds.: P. Diehl, E. Fluck, R. Kosfeld), Springer Publishers, Heidelberg, Berlin, New York, **1973**.
[24] B. Glaser, PhD Thesis, University of Munich, **1985**.
[25] B. Wrackmeyer, *Annual Reports on NMR Spectroscopy* **1985**, *16*, 73−186.

[26] B. Wrackmeyer, G. Kehr, H. Zhou, S. Ali, *Magn. Res. Chem.* **1996**, *34*, 921−928.
[27] M. Vosteen, PhD Thesis, University of Munich, **1999**.
[28] M. M. Crutchfield, C. M. Dungan, J. H. Letcher, V. Mark, J. R. van Wazer, *Topics in Phosphorus Chemistry* **1967**, *5*, 276.
[29] B. Eichhorn, H. Nöth, *Z. Naturforsch., Teil B* **2000**, *55*, 352−260.
[30] H. Nöth, I. Geisler, *Chem. Ber.* **1973**, *106*, 1943−1951.
[31] H. Fußstetter, G. Kopietz, H. Nöth, *Chem. Ber.* **1980**, *113*, 728−738.
[32] H. Nöth, S. Weber, *Z. Naturforsch., Teil B* **1983**, *38*, 1460−1465.
[33] A. Moezzi, M. M: Olmstead, P. P. Power, *J. Chem. Soc., Dalton Trans.* **1985,** 2949−234.
[34] D. Männig, H. Nöth, M. Schwartz, S. Weber, U. Wietelmann, *Angew. Chem.* **1985**, *97*, 979−980; *Angew. Chem. Int. Ed. Engl.* **1985**, *24*, 998−999.
[35] G. Johnson, J. Kane, R. Schaeffer, *J. Am. Chem. Soc.* **1970**, *92*, 7614−7615.
[36] M. P. Coles, D. C. Swenson, R. F. Jordan, V. G. Young Jr., *Oranometallics* **1997**, *16*, 5183−5194.
[37] J. Barker, N. C. Blacker, P. P. Phillips, N. N. Alcock, W. Errington, M. H. Wallbridge, *J. Chem. Soc., Dalton Trans.* **1996**, 431−437.
[38] S. Dagorne, R. F. Jordan, V. G. Young Jr., *Organometallics* **1999**, *18*, 4619−4623.
[39] Y. Zhou, D. S. Richeson, *Inorg. Chem.* **1996**, *35*, 2448−2451.
[40] A. Haaland, *Angew. Chem.* **1989**, *101*, 1017−1032; *Angew. Chem. Int. Ed. Engl.* **1989**, *28*, 992−1005.
[41] J. L. Atwood, G. A. Koutsantonis, F. C. Lee, C. L. Raston, *J. Chem. Soc., Chem. Commun.* **1994**, 91.
[42] S. J. Bryan, W. Clegg, R. Snaith, K. Wade, E. H. Wong, *J. Chem. Soc., Dalton Trans.* **1987**, 1223−1227.
[43] M. F. Lappert, P. P. Power, A. R. Sanger, R. C. Srivastava, *Metal and Metalloid Amides Synthesis − Structures, Physical and Chemical Properties*, Ellis Horwood Publ., New York, **1980**.
[44] B. Walfort, A. P. Leedham, Ch. A. Russell, *Inorg. Chem.* **2001**, *40*, 5668−5674.
[45] P. B. Hitchcock, H. A. Jasim, M. F. Lappert, H. D. Williams, *J. Chem. Soc., Chem. Commun.* **1986**, 1634−1636.
[46] K. M. Waggoner, M. M. Olmstead, P. P. Power, *Polyhedron* **1990**, *9*, 257−263.
[47] M. Mertz, W. Schwarz, D. Eberwein, J. Weidlein, H. Hess, H. P. Hausen, *Z. Anorg. Allg. Chem.* **1977**, *429*, 59−104.
[48] D. Arif, J. Bradley, *J. Chem. Soc., Chem. Commun.* **1985**, 783−784.
[49] K. Schmid, H. D. Hausen, K. W. Klinkhammer, J. Weidlein, *J. Organomet. Chem.* **1999**, *625*, 945−953.
[50] T. Gerstner, W. Schwarz, H. D. Hausen, *J. Organomet. Chem.* **1979**, *175*, 33−48.
[51] H. D. Hausen, K. Locher, J. Weidlein, *J. Organomet. Chem.* **1992**, *429*, C27−C32.
[52] H. H. Karsch, P. A. Schlüter, M. Reisky, *Eur. J. Inorg. Chem.* **1998**, 433−438.
[53] H. H. Karsch, P. A: Schlüter, F. Bienlein, M. Herke, E. Witt, A. Sladek, M. Heckel, *Z. Anorg. Allg. Chem.* **1990**, *583*, 7−16.
[54] A. Brandl, H. Nöth, *Chem. Ber.* **1988**, *121*, 1321−1328.
[55] R. Garbe, S. Wocadlo, H. C. Kang, W. Massa, K. Harms, K. Dehnicke, *Chem. Ber.* **1966**, *129*, 109−114.
[56] C. L. Raston, B. W. Shelton, V. H. Tolhurst, A. H. White, *J. Chem. Soc., Dalton Trans.* **2000**, 1279.
[57] C. Enzinger, F. Weller, K. Dehnicke, *Z. Naturforsch., Teil B* **1988**, *43*, 1119−1124.
[58] H. W. Roesky, K. Hübner, M. Noltemeyer, M. Schäfer, *Angew. Chem. Int. Ed. Engl.* **1991**, *103*, 856−857, *Angew. Chem. Int. Ed. Engl.* **1991**, *30*, 860−861.
[59] SMART and SAINT, Bruker Analytical Instruments, Madison, Version 5.1.
[60] SADABS, Absorption correction as implemented in SHELXTL, Bruker Analytical Instruments. Madison, Version 5.1.
[61] SHELX97, G. W. Sheldrick, University of Göttingen, **1997**.

Received February 13, 2004
Early View Article
Published Online July 21, 2004

